ARMY RESEARCH LABORATORY

Comparison of the Inversion Periods for Polarimetric and Conventional Long-wave IR (LWIR) Imagery

by M. Felton, K. P. Gurton, L. E. Roth, J. L. Pezzaniti, and D. B. Chenault

ARL-TR-4931 **August 2009**

NOTICES

Disclaimers

The findings in this report are not to be construed as an official Department of the Army position unless so designated by other authorized documents.

Citation of manufacturer's or trade names does not constitute an official endorsement or approval of the use thereof.

Destroy this report when it is no longer needed. Do not return it to the originator.

Army Research Laboratory
Adelphi, MD 20783-1197

ARL-TR-4931 **August 2009**

Comparison of the Inversion Periods for Polarimetric and Conventional Long-wave IR (LWIR) Imagery

M. Felton and K. P. Gurton
Computational and Information Sciences Directorate, ARL

L. E. Roth
U.S. Army Armament Research and Development Engineering Center

J. L. Pezzaniti and D. B. Chenault
Polaris Sensor Technologies, Inc.

REPORT DOCUMENTATION PAGE

Form Approved
OMB No. 0704-0188

1. REPORT DATE *(DD-MM-YYYY)*	2. REPORT TYPE	3. DATES COVERED (From - To)
August 2009	Summary	May 2009 to July 2009

4. TITLE AND SUBTITLE
Comparison of the Inversion Periods for Polarimetric and Conventional Long-wave IR (LWIR) Imagery

5a. CONTRACT NUMBER

5b. GRANT NUMBER

5c. PROGRAM ELEMENT NUMBER

6. AUTHOR(S)
M. Felton, K. P. Gurton, L. E. Roth, J. L. Pezzaniti, and D. B. Chenault

5d. PROJECT NUMBER

5e. TASK NUMBER

5f. WORK UNIT NUMBER

7. PERFORMING ORGANIZATION NAME(S) AND ADDRESS(ES)
U.S. Army Research Laboratory
ATTN: RDRL-CIE
2800 Powder Mill Road
Adelphi, MD 20783-1197

8. PERFORMING ORGANIZATION REPORT NUMBER
ARL-TR-4931

9. SPONSORING/MONITORING AGENCY NAME(S) AND ADDRESS(ES)

10. SPONSOR/MONITOR'S ACRONYM(S)

11. SPONSOR/MONITOR'S REPORT NUMBER(S)

12. DISTRIBUTION/AVAILABILITY STATEMENT
Approved for public release; distribution unlimited.

13. SUPPLEMENTARY NOTES

14. ABSTRACT
We report the results of a multi-day diurnal study in which radiometrically calibrated polarimetric and conventional thermal imagery is recorded in the long-wave IR (LWIR) to identify/compare the respective time periods in which minimum target contrast is achieved, e.g., thermal inversion periods are typically experienced during dusk and dawn. Imagery is recorded with a polarimetric IR sensor employing a 324x256 microbolometer array using a spinning achromatic retarder to perform the polarimetric filtering. The images used in this study include the S_0, normalized S_1, and normalized S_2 Stokes images and the degree of linear polarization (DOLP) images of a scene containing military vehicles and the natural background. In addition, relevant meteorological parameters measured during the test period include air temperature, ambient loading in the LWIR, relative humidity, and cloud cover, height and density. The data shows that the chief factors affecting polarimetric contrast are the amount of thermal emission from the objects in the scene and the abundance of LWIR sources in the optical background. In addition, we found that contrast between targets and background within polarimetric images often remains relatively high during periods of low thermal contrast.

15. SUBJECT TERMS
Polarimetric imaging, thermal imaging, microbolometer, target contrast, inversion periods

16. SECURITY CLASSIFICATION OF:			17. LIMITATION OF ABSTRACT	18. NUMBER OF PAGES	19a. NAME OF RESPONSIBLE PERSON
a. REPORT	b. ABSTRACT	c. THIS PAGE			M. Felton
Unclassified	Unclassified	Unclassified	UU	28	19b. TELEPHONE NUMBER (*Include area code*) (301) 394-2618

Standard Form 298 (Rev. 8/98)
Prescribed by ANSI Std. Z39.18

Contents

List of Figures

List of Tables

Acknowledgments

This work was accomplished using data from the Hyperspectral and Polarimetric Target Detection Program at the Precision Armament Laboratory (PAL) Tower at the Armament Research and Development Engineering Center (ARDEC) with the help of Mr. Joao Romano (Program Manager) and Mr. Mark Woolley (PAL Manager).

1. Introduction

Thermal imagers have been established as the primary tool used in military and security activities that involve surveillance, targeting and tracking, and nighttime operations. Unlike image intensification (I^2) devices, which depend on ambient light levels, thermal imagers exploit the fact that all objects with a temperature above absolute 0 K emit thermal radiation by creating a pseudo image of the scene based on this thermal emission. The two thermal imaging windows are the mid-infrared (IR), 3–5 μm, and the long-wave IR (LWIR), 8–14 μm, both chosen for the relatively low amounts of absorption from atmospheric species such as carbon dioxide (CO_2) and water (H_2O).

Contrast between the objects within a thermal image is determined by their effective temperatures, which are a function of their true temperature and their emissivity, a characteristic of an object that describes how efficiently it radiates absorbed energy as compared to a blackbody. If there is no thermal contrast between a target and its background, it cannot be seen in a thermal image. The diurnal cycles of the thermal properties of both manmade and natural objects tend to bring about periods of low contrast within thermal images, often referred to as thermal crossovers or inversion periods (*1*). These inversion periods tend to occur during periods of rapidly changing temperatures, such as sunrise and sunset, but may occur at any time throughout the day, depending both on temperature differences between objects and their backgrounds and environmental factors such as solar loading. A technology that enhances conventional thermal imaging should extend its operational ability into these periods of thermal inversion.

1.1 Thermal Polarimetric Imaging

Thermal polarimetric imaging has been proposed as a method to enhance conventional thermal imaging (*2*). It creates images of a scene that are based on the states of polarization of the IR light emitted or reflected from the objects within the scene. An object's polarimetric signature is a function of its surface geometry and roughness. Due to the different geometrical and roughness features of objects constituting the natural background and manmade objects, the polarization states of the emitted and reflected thermal light can be used as a discriminator between objects of interest and background clutter. By using the additional information in the form of polarization, it is possible to obtain an image of a scene that has polarimetric contrast between objects and their backgrounds, despite the fact that there is no thermal contrast.

Just as there are environmental factors that affect thermal contrast, there are also environmental factors that affect polarimetric contrast. The most significant of these factors involves sources of IR radiation in what has been referred to as the optical background, which is defined as the sources of IR radiation that are not necessarily visible within the scene but still reflect IR

radiation off of an object and into the field of view (FOV) of the camera (*3*). The optical background can become partially polarized upon reflection and act as a competing component to the emitted polarized light. Polarized emitted and reflected light are often orthogonal to each other, because the emitted polarized light tends to be in the direction parallel to the surface normal while light polarized upon reflection tends to be in the direction parallel to the reflecting surface. When the two superpose, the effect can be a reduction in the magnitude of the polarimetric signature of an object. Potential sources of optical background radiation may include vehicles, buildings, trees, clouds, and water vapor.

This study compares the temporal occurrence of conventional thermal inversion periods to that of polarimetric and correlates these inversions with environmental factors. If there are significant periods of time in which contrast within polarimetric images are present while conventional thermal contrast has been lost, then it can be concluded that polarimetric imaging can enhance conventional thermal imaging.

2. Experiment

2.1 Polarimetric Sensor

The sensor used is a LWIR microbolometer-based rotating retarder imaging polarimeter developed by Polaris Sensor Technologies, Inc., Huntsville, AL (figure 1) (*4*). It operates by capturing images sequentially in time, each at a different orientation of the rotating retarder. Together, the retarder and linear polarizer act as a polarization state analyzer for the light forming the image. Using the data reduction matrix method, the Stokes vectors are calculated, which completely characterize the polarization states of the light from the scene. Table 1 lists the sensor specifications and table 2 provides definitions of the data products used in this study.

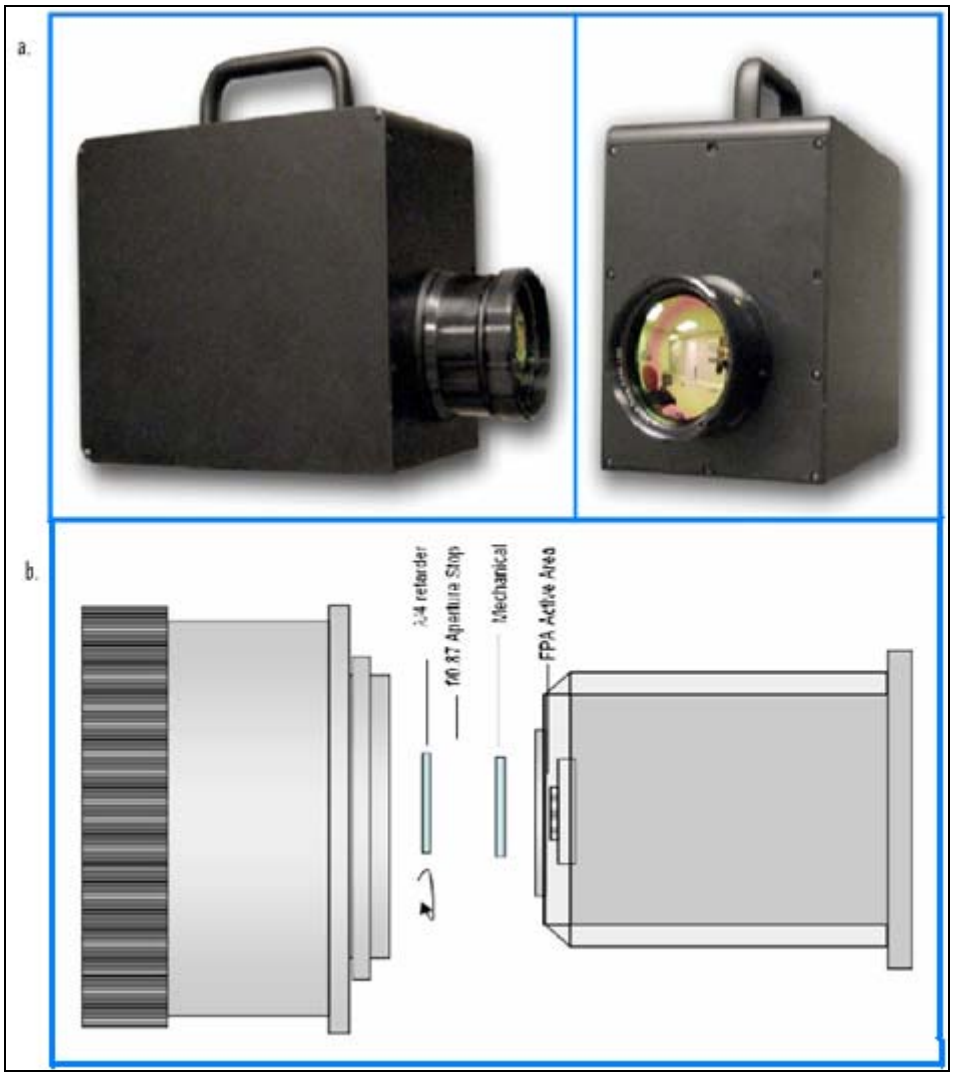

Figure 1. a. Image of polarimetric sensor and b. optical layout of the spinning retarder, microbolometer-based sensor.

Table 1. Specifications for the polarimetric sensor.

Parameter	Value
Waveband	7.5–13.5 µm
FOV	13.7° x 11.0°
Objective focal length	50 mm
Total FPA size	324 x 256
Frame rate	30 frames per second

Note: FPA = focal plane array

Table 2. Polarimetric sensor data products.

Measured image	Description
S_0	Radiance image, W/cm^2-sr
S_1	Horizontally polarized radiance minus vertically polarized radiance, W/cm^2-sr
S_1/S_0	S_1 image normalized by radiance image, S_0
S_2	45° polarized radiance minus 135° polarized radiance, W/cm^2-sr
S_2/S_0	S_2 image normalized by radiance image, S_0
DOLP	Degree of linear polarization, $\frac{\sqrt{S_1^2 + S_2^2}}{S_0}$

A four-point non-uniformity correction was done to correct for non-uniformities in the FPA and slight nonlinearity in the sensor response. The temperatures were chosen to encompass the range of temperatures of the objects in the scene that were expected to be encountered during the study. The polarimetric calibration was carried out using a wire-grid polarizer on a barium fluoride (BaF_2) substrate that was back illuminated by a blackbody source and canted at an angle so that it was front illuminated by a large roughened black plate uniformly at room temperature so that reflected radiance from the face of the polarizer was kept constant.

2.2 Field Test Site

The test was conducted at the Precision Armaments Laboratory located in Picatinny Arsenal, NJ. The camera was situated on the sixth floor of a tower (approximately 200 ft high) looking out of the windows towards the target site, which was at approximately 0.5 km in range and consisted of two military vehicles and natural backgrounds including grass, brush, and trees (figures 2 and 3). In addition to the 200-ft elevation of the sixth floor of the tower, the tower itself was situated on top of a ridge approximately 150 ft above the target site.

Figure 2. Precision Armaments Laboratory tower with elevator that housed the polarimetric sensor situated on the sixth floor.

Figure 3. Target site consisting of two military vehicles and a natural background. The test was carried out May 12–15, 2009, but this image was taken in the preceding fall. Therefore, during the test, the grass was alive and thick and the bushes and trees contained leaves.

Environmental measurements available at the target site include air temperature, relative humidity, ceilometer data, and pyrgeometer (precision infrared radiometer [PIR]) data. The ceilometer provides real-time reports of cloud bases and depths directly above the ceilometer and determines cloud cover by using a weighted average of 30-s cloud hit reports over a 30-min period. The pyrgeometer measured ambient LWIR radiation from 3−50 μm within a 2π steradian FOV.

The data acquisition clocks for the environmental data and the camera were synced to ensure coincident data. The temporal resolution of the data are as follows: air temperature, relative humidity and pyrgeometer – 2 s; ceilometer – 10 s; and camera – 10 min. Data was acquired continuously beginning at 10:00 on May 12, 2009, and ended at 09:00 on May 15, 2009.

2.3 Image Analysis

A contrast-based study was performed between the military vehicles and their immediate backgrounds. The data products used in this study include S_0, normalized S_1, normalized S_2, and degree of linear polarization (DOLP). Because some of these data products are measured in different units and are of different magnitudes, the analysis was performed on standardized versions of these images (*5, 6*). In other words, each image had its mean subtracted and was normalized by its standard deviation. This makes it possible to directly compare the contrasts for all of the data products. Using temporal sequences of co-registered images, regions of interest were defined for the targets and their backgrounds and the mean values were calculated for each data product at each time in the series. The contrast is defined as the absolute value of the difference between the mean target value, μ_t', and the mean background value, μ_b', where the prime indicates that the means were calculated using standardized images:

$$contrast = \left|\mu_t' - \mu_b'\right|. \tag{1}$$

Because standardizing the images gives them unitless values, the contrast defined by equation 1 is also unitless.

Data for two targets (military vehicles) are used in the analysis. One target was directly facing the tower while the other was oriented at a 45° angle relative to the tower (figure 4). These two orientations required different strategies for choosing the regions of interest. Most of the surfaces of the target in figure 4a are oriented in the same direction relative to the FOV of the camera. Therefore, widely varying magnitudes of polarimetric signatures due to diversity of surface geometry minimally affect the target's mean signatures. On the other hand, the target oriented at 45° (figure 4b) has multiple surfaces oriented in different directions, and therefore, each one preferentially produces states of polarization that can lead to misleading signatures when averaged together. For this target, two separate regions of interest were used, each corresponding to a prominent surface.

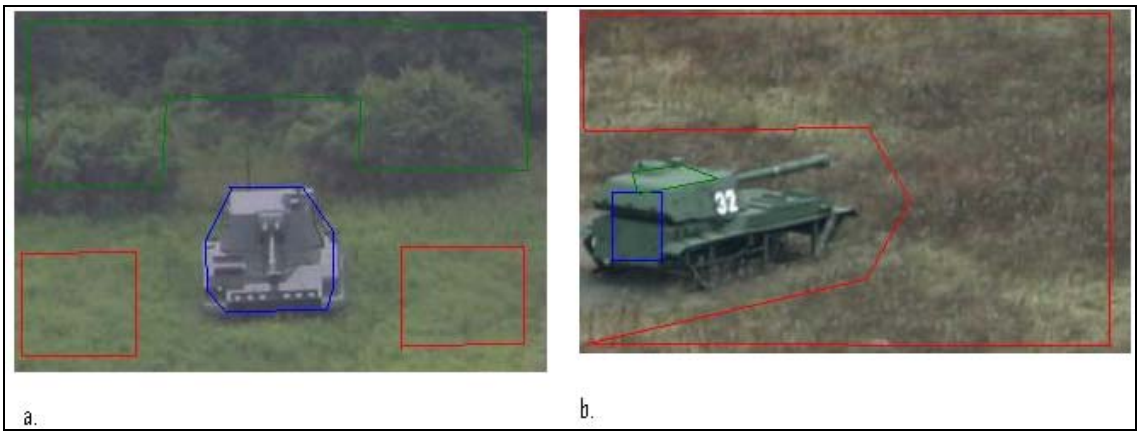

Figure 4. a. Target 1 and its natural background. The target, grass, and trees regions of interest correspond to the blue, red, and green boxes, respectively. b. Target 2 and its natural background. The back and top of the target and the grass regions of interest correspond to the blue, green, and red boxes, respectively.

Examples of contrast values calculated using equation 1 and their corresponding images are shown in figure 5. The contrasts were calculated for the S_0 images of the scene in figure 4a taken at three different times of the day. Because this scene has two different natural backgrounds, one is chosen at a time to calculate the contrast between the target and the chosen background. In the case of figure 5, the grass background is used to calculate the contrast.

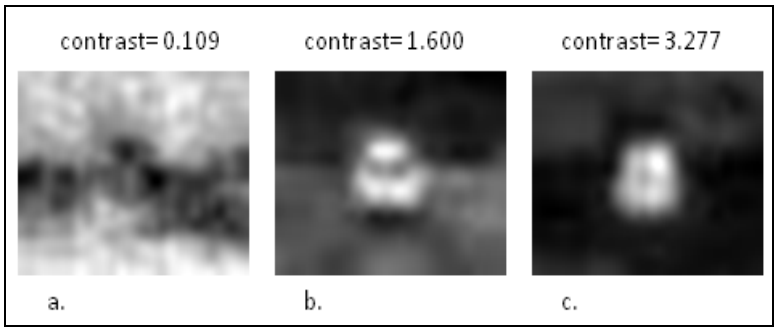

Figure 5. Example contrast values comparing the target to the grass and the corresponding S_0 image taken at a. 07:00, b. 11:00, and c. 19:00.

3. Results

The results are presented in the form of diurnal contrast plots (calculated using equation 1) and the corresponding environmental data. The ceilometer data is omitted because the cloud information can be obtained from the pyrgeometer (PIR) data. A direct comparison of ceilometer and pyrgeometer data revealed that the baseline reading for a cloudless daytime sky

was roughly 275–280 W/m^2. Any value higher than this typically indicates the presence of clouds such that the higher the value, the thicker the cloud cover. During this study, sunrise and sunset occurred at roughly 05:00 and 20:00, respectively.

3.1 Scene in Figure 4a

Figures 6–9 present the diurnal contrast for the target in figure 4a against its background of grass and trees for May 12, 13, 14, and 15, 2009, respectively. For this scene, it was consistently found that DOLP is dominated by S_1 because the magnitude of S_2 was generally half that of S_1. Therefore, the DOLP contrast often mimics the S_1 contrast. On the other hand, the S_2 contrast was found to mimic the S_0 contrast. From the FOV of the sensor, there are not many facets of the target in figure 4a that are capable of producing large amounts of 45° or 135° polarized light, namely surfaces oriented at 45° or 135° with the cold sky as an optical background. Therefore, the S_2 measured by the sensor is mainly due to emission and affected by cloud cover to a lesser extent than S_1 and DOLP.

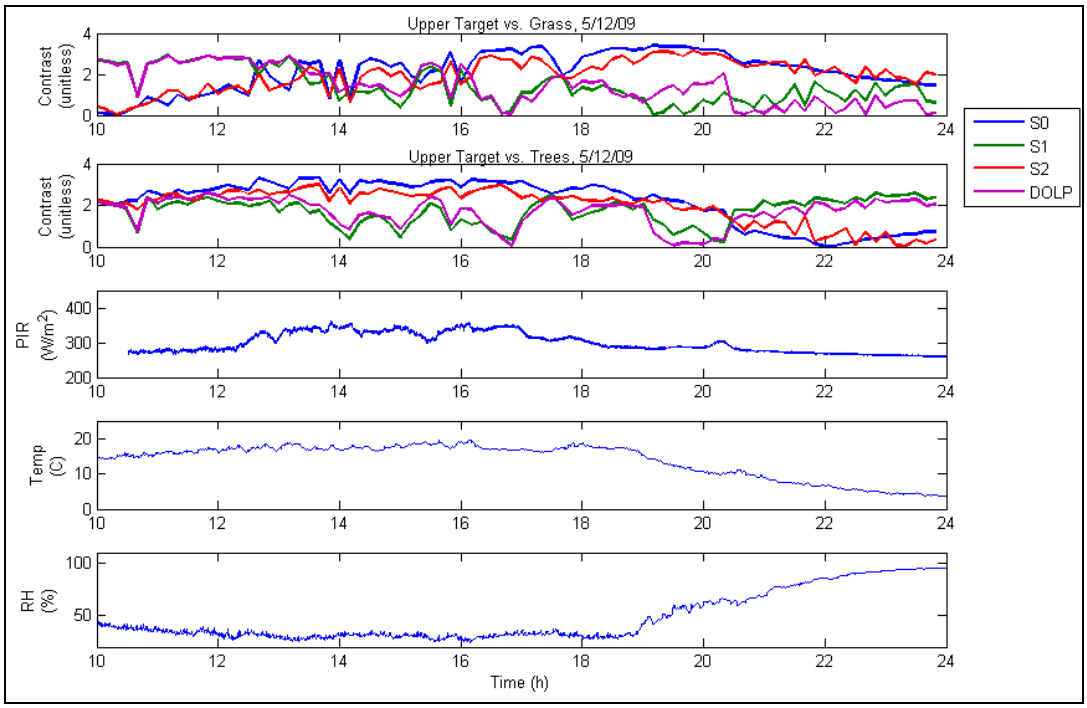

Figure 6. Diurnal contrast for the target in figure 4a compared to its two backgrounds, grass and trees, on May 12, 2009.

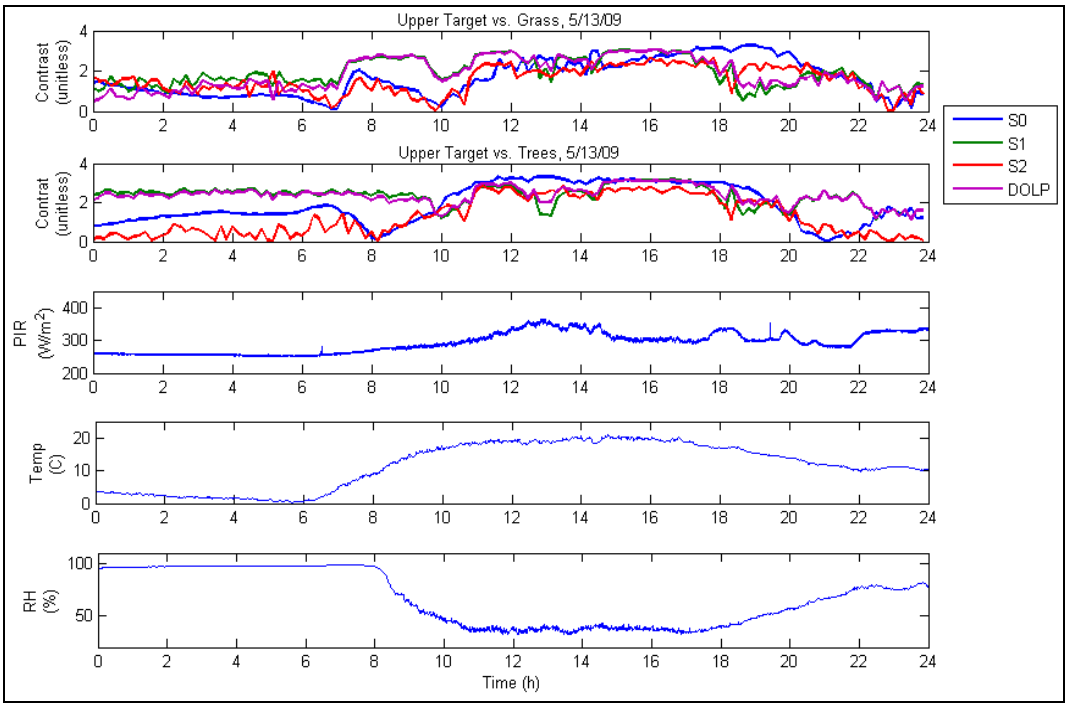

Figure 7. Diurnal contrast for the target in figure 4a compared to its two backgrounds, grass and trees, on May 13, 2009.

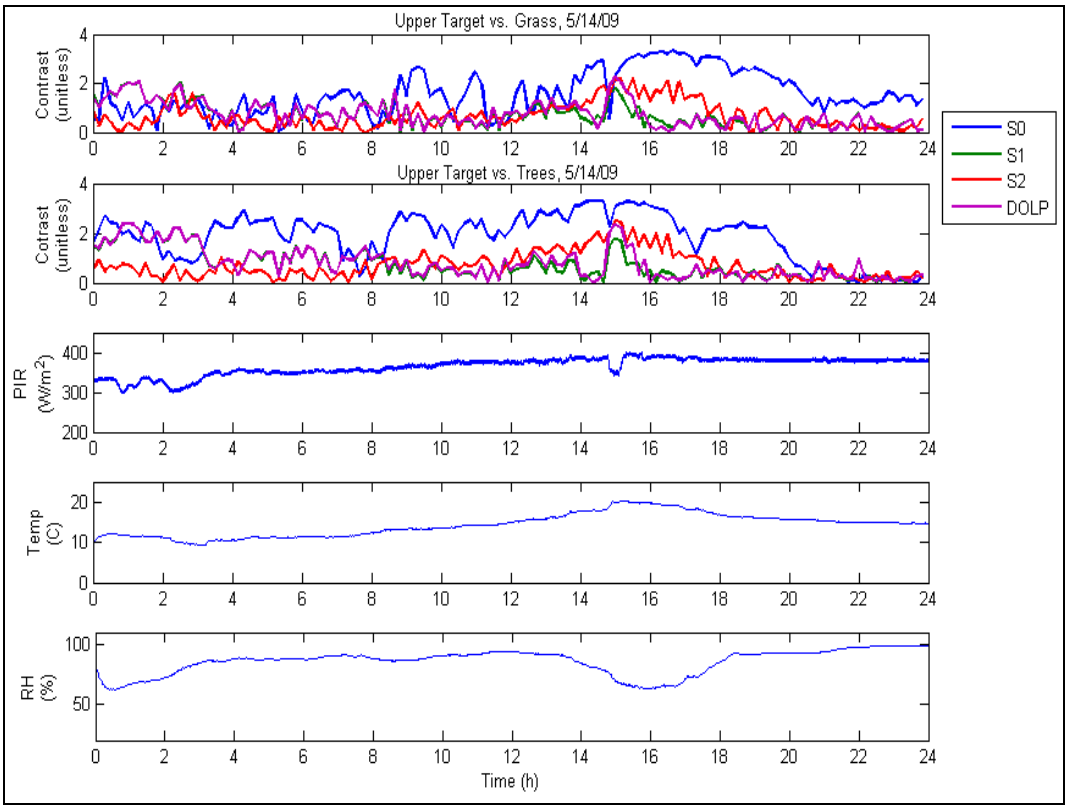

Figure 8. Diurnal contrast for the target in figure 4a compared to its two backgrounds, grass and trees, on May 14, 2009.

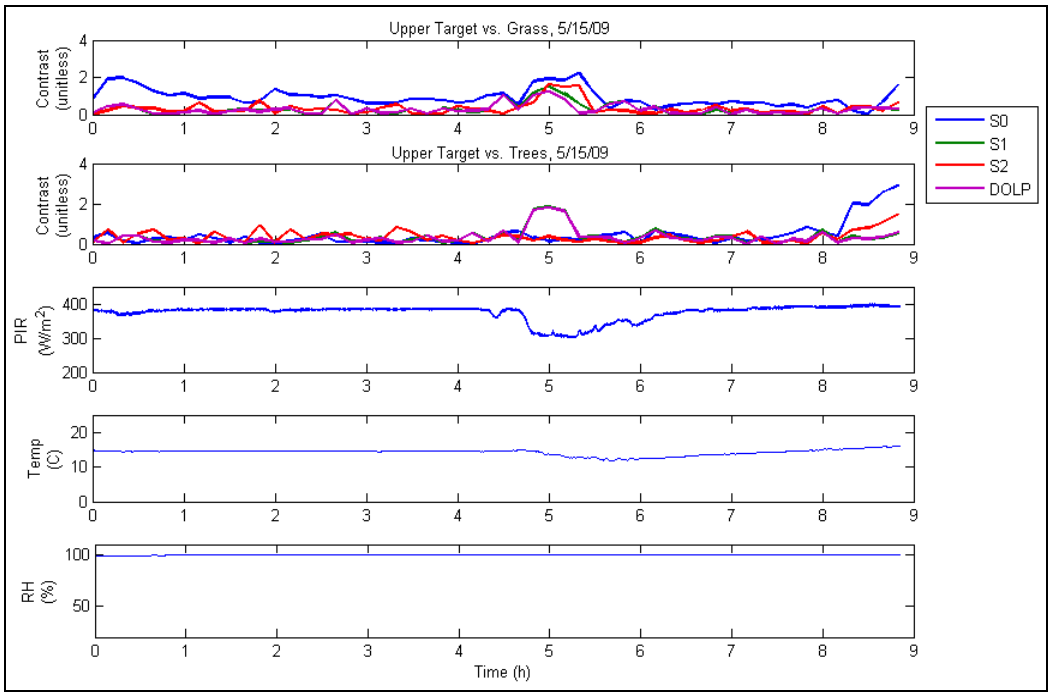

Figure 9. Diurnal contrast for the target in figure 4a compared to its two backgrounds, grass and trees, on May 15, 2009.

May 12 and 13 were similar days in that the morning skies were clear while the afternoon skies were partly cloudy at times. In addition, the temperature and relative humidity were inversely proportional to each other on both days. The S_0 and S_2 contrasts were best at higher temperatures. Thermal inversions occurred during times of rapidly changing temperatures in the morning and at night. At 10:00 on May 12 and 07:00, 10:00, and 23:00 on May 13, there were thermal inversions between the target and the grass, as can be seen from the S_0 contrast curves in figures 6 and 7 during these times. In additional, thermal inversion periods were experienced between the target and the trees at 22:00 on May 12 and at 08:00 and 21:00 on May 13. With the exception of 23:00 on May 13 between the target and the grass, polarimetric contrast, namely in S_1 and DOLP, remained high during the periods of thermal inversion that occurred on the first two days of the test. The primary factor effecting S_1 and DOLP contrast was sources of LWIR optical background, which came in two forms: the presence of clouds in the sky and the presence of a truck that was temporarily driven into the scene. Inversions correlated to cloud cover occurred in these data products on May 12, while the presence of clouds had a milder impact on May 23, often reducing contrast as opposed to eliminating it. Reduced contrast in S_1 and DOLP due to the truck is evident at 10:40 on May 12 and from 09:50–10:50 on May 13. The truck was situated approximately 15 ft in front and to the right of the target. Extra care was taken to ensure that the regions of interest for the grass did not include any portion of the truck. Figure 10a shows the S_0 image of the target site at 10:00, which is after the truck has been introduced into the scene. Figure 10b and c are normalized S_1 images that focus on the upper target at 09:30 (before the truck was introduced into the scene) and 10:00 (after the truck was

introduced into the scene), respectively. The black, rectangular shape in the bottom right-hand corner of figure 10c is the back portion of the top of the truck. These images are displayed on the same scale and illustrate the decreases in contrast in the normalized S_1 images between the target and its background as shown in the S_1 curve of figure 7, namely during the time period 09:50–10:50.

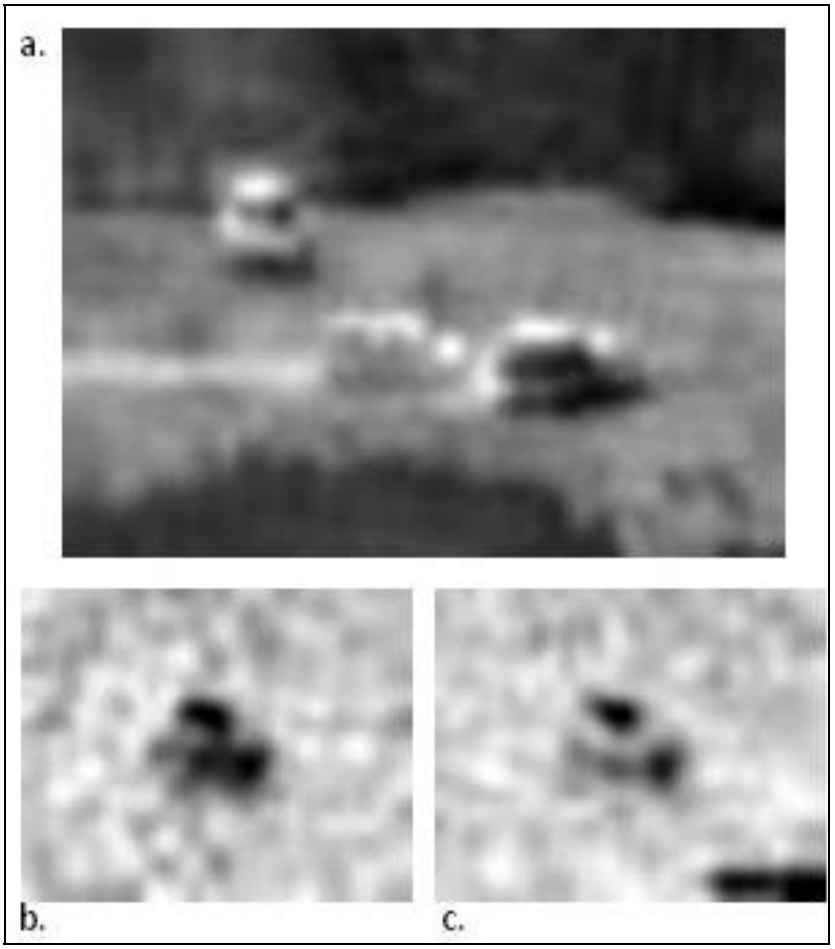

Figure 10. a. S_0 image of the target site at 10:00 on May 13 with the truck introduced into the scene. b. Normalized S_1 image of the upper target at 09:30 before the truck was introduced into the scene. c. Normalized S_1 image of the upper target at 10:00 after the truck was introduced into the scene.

Inclement weather moved into the Picatinny area in the early morning hours of May 14 and there were intermittent periods of light rain up until the early afternoon. During this time, there was thick cloud cover as reflected in the PIR plot of figure 8. The fluctuations in thermal contrast are caused by the periods of light rain, which has the effect of wetting the surfaces in the scene causing them all to appear the same temperature. In addition, there was a slight break in the cloud cover at 15:00, which caused the scene to heat. The S_0 contrast initially is reduced, as the target and its backgrounds approach the same temperature due to different rates of heating. Eventually, the S_0 contrast improves as the effective temperatures of the target and its

backgrounds reach their respective levels. This same lag in improved contrast is not experienced by the polarimetric data products, because their contrast mainly depends on the optical background. As can be seen from the PIR plot at 15:00 in figure 8, there is a slight reduction in ambient LWIR due to a break in the clouds, resulting in a temporary improvement in the contrast of the polarimetric data products. Conditions remained the same throughout the night and through the next morning. Contrast remains low in all data products due to the static temperatures and constant cloud cover until sunrise just before 05:00 when there was a slight break in the clouds. Temporary contrast appears between the target and the grass in all data products and only in S_1 and DOLP between the target and the trees. At 05:30, thick fog descended onto the target site until just after 08:00. During this time, all contrast was lost.

3.2 Scene in Figure 4b

Figures 11–14 present the diurnal contrast for the target in figure 4b against its background of grass for May 12, 13, 14, and 15, 2009, respectively. Recall that the contrasts were calculated using two different prominent facets of the target in figure 4b, as opposed to the entire target, so that cancellation effects could be kept to a minimum. Unlike the target in figure 4a, the target in figure 4b has a facet that is oriented in such a way that it is capable of producing larger amounts of S_2, namely the back of the target. This is reflected in the contrast plots in figures 11 and 12. On both of these days, the contrast for the back of the target is greatest in the S_2 images during clear sky conditions in the morning hours when the back of the target is receiving more direct illumination from the sun while reflecting the cold sky. When clouds enter the sky, the S_2 contrast for the back of the tank is reduced. The S_1 and DOLP contrast for the back of the target is generally lower than the S_2 contrast, while the S_0 contrast was the highest in the afternoons on both days.

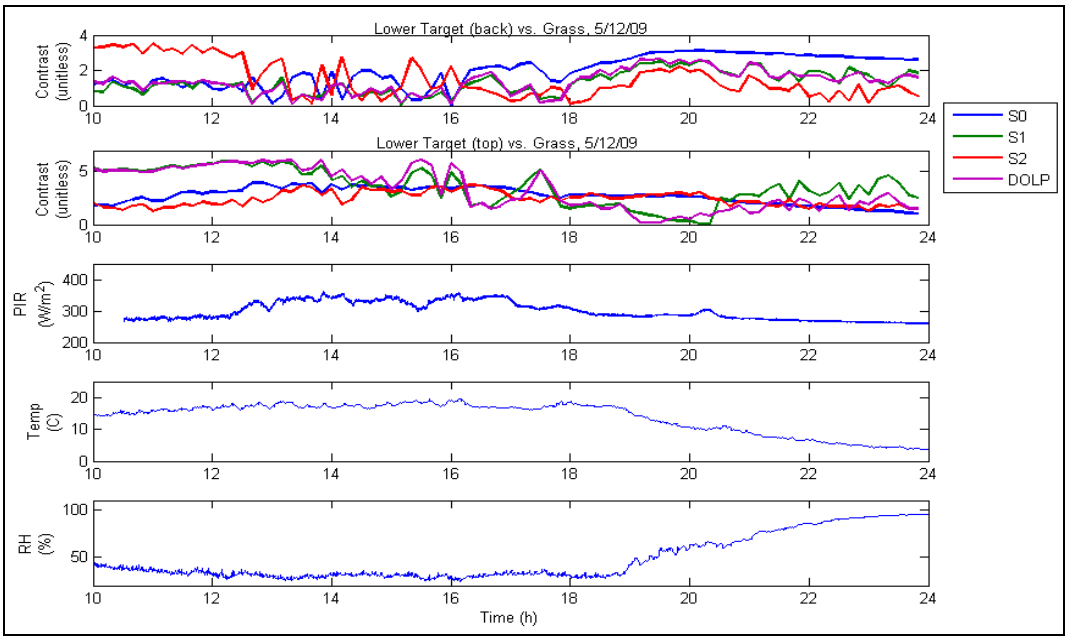

Figure 11. Diurnal contrast for the target in figure 4b and its background of grass on May 12, 2009.

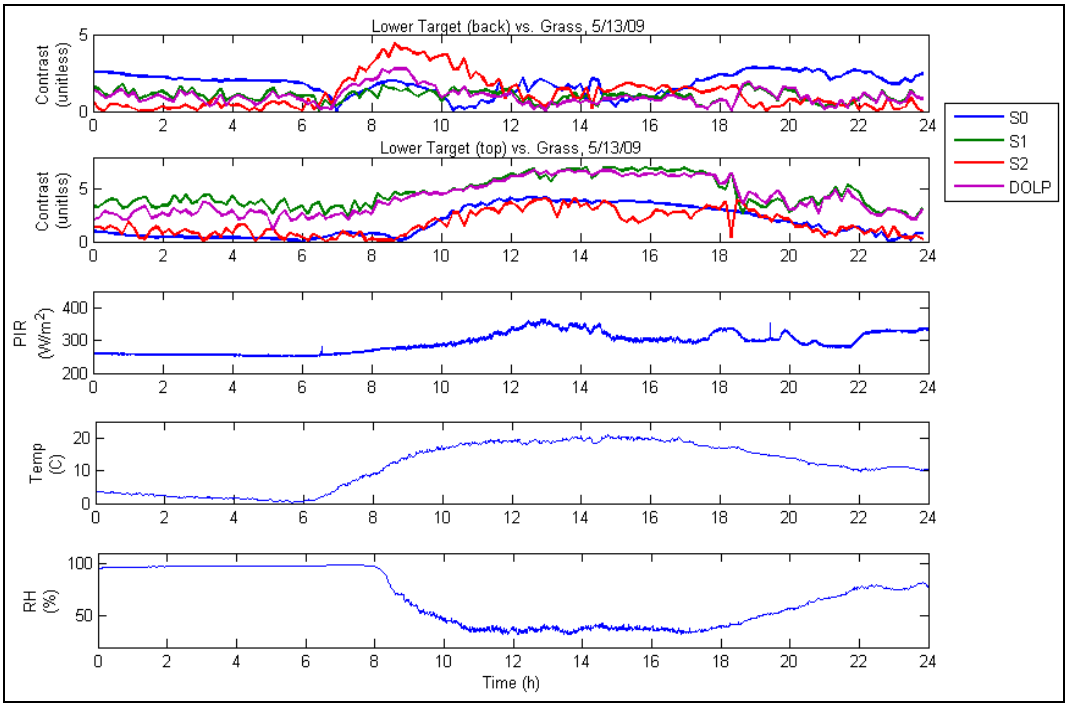

Figure 12. Diurnal contrast for the target in figure 4b and its background of grass on May 13, 2009.

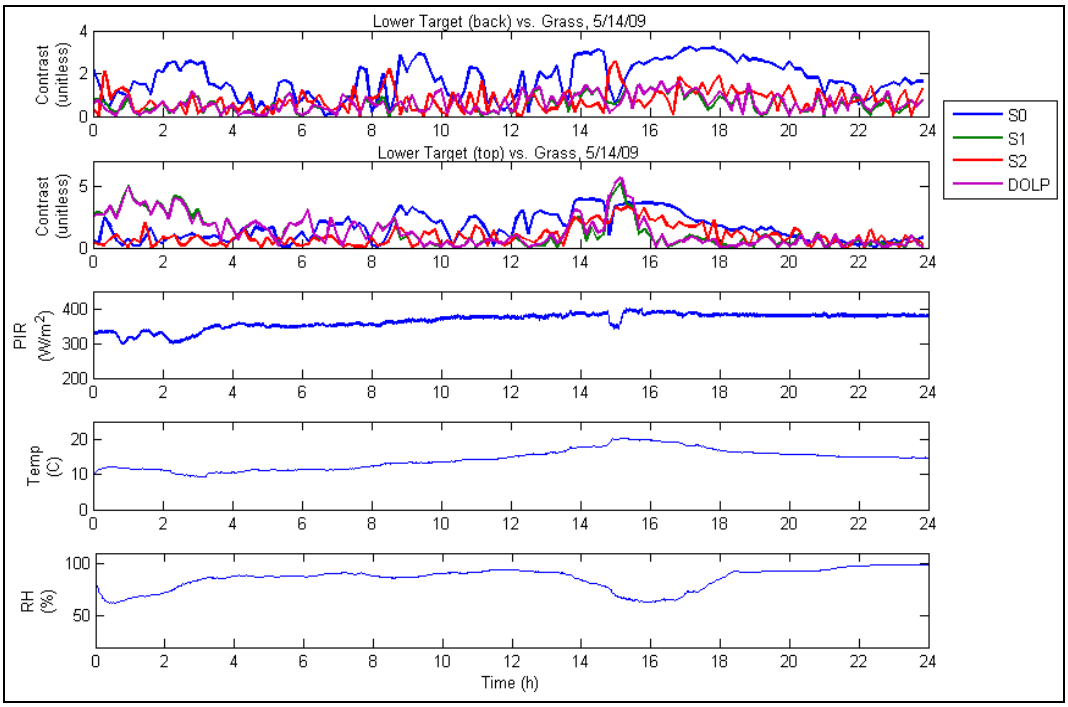

Figure 13. Diurnal contrast for the target in figure 4b and its background of grass on May 14, 2009.

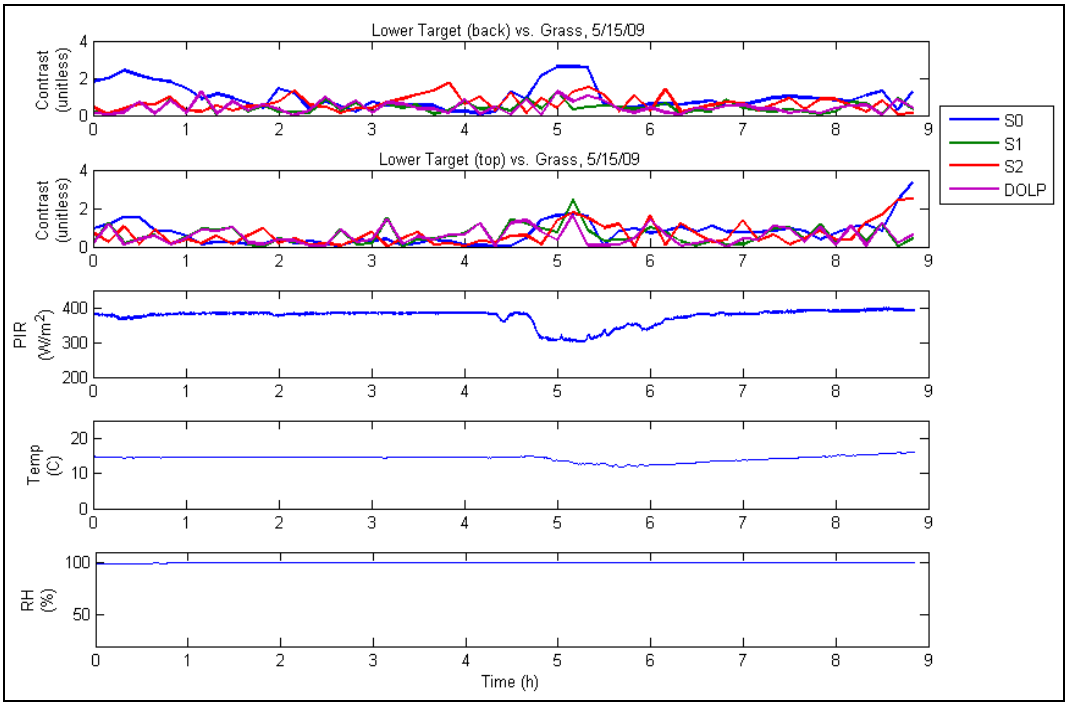

Figure 14. Diurnal contrast for the target in figure 4b and its background of grass on May 15, 2009.

On May 12, the contrast for the top of the target in the S_1 and DOLP images was much higher than for S_0 and S_2 under clear sky conditions. The presence of clouds acted as a source of LWIR and therefore produced a reflected component off of the target that competed with the target's

emitted S_1 and DOLP signatures. On May 13, the contrast in the S_1 and DOLP images were consistently higher than that of S_0 and S_2. The contrast was again modulated by the presence of clouds but to a lesser extent than on the previous day. Most importantly, during the period of low thermal contrast observed from 00:00 to 09:00 on May 13, there was significant contrast in the S_1 and DOLP images.

The effect of the thick cloud cover and periods of light rain on May 14 can be seen in figure 13 for the back of the target as the overall poor contrast in all polarimetric images and the intermittent contrast present thermally. The S_2 contrast peaks at 15:00 at the exact time that there is a break in the clouds, indicating that the lack of contrast was due to the LWIR optical background provided by the clouds. Similarly, for the top of the target, each time there was a slight break in the clouds, i.e., 00:00–04:00 and 15:00, there was a return of the contrast to the S_1 and DOLP images. The results were similar during the conditions of thick cloud cover and fog experienced on the morning of May 15. The slight break in the clouds around sunrise allowed contrast to briefly return in the S_0 images of the back of the target and in all of the images for the top of the target. The fog eventually sets in and destroys all contrasts.

4. Conclusions

In this study, the temporal occurrence of conventional thermal and polarimetric inversions was examined as well as their correlations to environmental factors. Imagery was recorded with a polarimetric IR sensor employing a 324x256 microbolometer array using a spinning achromatic retarder to perform the polarimetric filtering. The images used in this study included the S_0, normalized S_1, and normalized S_2 Stokes images and the DOLP images of scenes containing military vehicles and the natural background. In addition, relevant meteorological parameters measured during the test periods included air temperature, ambient loading in the LWIR, relative humidity, and cloud cover, height and density.

This study revealed that during most thermal inversion periods, there remains polarimetric contrast between at least some facet of the target, and in many cases, the whole target, and its background. In addition, the data shows that the chief factors affecting polarimetric contrast are the amount of thermal emission from the objects in the scene and the abundance of LWIR sources in the optical background.

These findings suggest that conventional thermal imagery can be enhanced by incorporating polarimetric information. The typical thermal inversions can affect contrast for up to 2 h at a time, reducing their effectivity and jeopardizing the success of military and security missions. The ability of polarimetric imaging to enhance conventional thermal imaging is limited by susceptibility to the optical background. If a polarmetrically enhanced thermal imager is being used during a mission under conditions in which there are significant optical background

sources, then the performance of the system will reduce to that of a conventional thermal system. In the absence of sources of LWIR optical background, the system will greatly improve the detection of objects of interest against natural backgrounds.

5. References

1. Shumaker, D. L.; Wood, J. T.; Thacker, C. R. *Infrared Imaging Systems Analysis*; DCS Corporation, Alexandria, VA, 1993, 2-45–2-49.

2. Tyo, J. S.; Goldstein, D. L.; Chenault, D. B.; Shaw, J. A. Review of Passive Imaging Polarimetry for Remote Sensing Applications. *App. Optics* **2006**, *45* (22), 5453–5469.

3. Tyo, J. S.; Ratliff, B. M.; Boger, J. K.; Black, W. T.; Bowers, D. L.; Fetrow, M. P. The Effects of Thermal Equilibrium and Contrast in LWIR Polarimetric Images. *Optics Exp.* **2007**, *15* (23), 15161–15167.

4. Pezzaniti, J. L.; Hyatt, B.; Reinhardt, J. *Systems Users Manual: LWIR Rotating Retarder Imaging Polarimeter*, 2008.

5. Dillon, W. R.; Goldstein, M. *Multivariate Analysis: Methods and Applications*; John Wiley & Sons, New York, Chichester, Brisbane, Toronto, and Singapore, 10–13, 1984.

6. Felton, M.; Gurton, K. P.; Ligon, D.; Raglin, A. D*iscrimination of Objects Within Polarimetric Imagery Using Principle Component and Cluster Analysis*; ARL-TR-4216; U.S. Army Research Laboratory: Adelphi, MD, 2007.

List of Symbols, Abbreviations, and Acronyms

ARDEC	Armament Research and Development Engineering Center
BaF_2	barium fluoride
CO_2	carbon dioxide
DOLP	degree of linear polarization
FOV	field of view
H_2O	water
I^2	image intensification
IR	infrared
LWIR	long-wave IR
PAL	Precision Armament Laboratory
PIR	precision infrared radiometer

NO. OF COPIES	ORGANIZATION
1 ELEC	ADMNSTR DEFNS TECHL INFO CTR ATTN DTIC OCP 8725 JOHN J KINGMAN RD STE 0944 FT BELVOIR VA 22060-6218
1	DARPA ATTN IXO S WELBY 3701 N FAIRFAX DR ARLINGTON VA 22203-1714
1 CD	OFC OF THE SECY OF DEFNS ATTN ODDRE (R&AT) THE PENTAGON WASHINGTON DC 20301-3080
1	US ARMY ABERDEEN TEST CENTER ATTN TEDT AT WFT F CARLEN 400 COLLERAN ROAD ABERDEEN PROVING GROUND MD 21005-5009
1	US ARMY ARMAMENT RSRCH AND DEVELOPMENT ENGINEERING CTR ATTN AMSRD AAR MEF S L E ROTH BLDG 407 PICATINNY ARSENAL NJ 07806-5000
1	US ARMY CECOM RDEC NVESD ATTN AMSRD CER NV ST SIP J HOWE 10221 BURBECK RD STE 430 FT BELVOIR VA 22060-5806
1	US ARMY INFO SYS ENGRG CMND ATTN AMSEL IE TD A RIVERA FT HUACHUCA AZ 85613-5300
1	COMMANDER US ARMY RDECOM ATTN AMSRD AMR W C MCCORKLE 5400 FOWLER RD REDSTONE ARSENAL AL 35898-5000
1	US ARMY RDECOM ARDEC ATTN AMSRD AAR AEP S J ROMANO BLDG 407 PICATINNY ARSENAL NJ 07806-5000

NO. OF COPIES	ORGANIZATION
1	US ARMY TARDEC ATTN AMSRD TAR MS 263 G GRANT 6501 EAST 11 MILE RD WARREN MI 48397-5000
1	AFRL/RYJT ATTN R T MACK 2241 AVIONICS CIRCLE BLDG 620 WRIGHT-PATTERSON AFB OH 45433-7320
1	AFRL/VS ATTN T R CAUDILL 3550 ABERDEEN AVE SE BLDG 423 KIRTLAND AFB NM 87117
1	AFRL/VSS ATTN M J DUGGIN 3550 ABERDEEN AVE SE KIRTLAND AFB NM 87117
1	USAFRL-VSSS ATTN M FETROW 3550 ABERDEEN SE KIRTLAND AFB NM 87117
1	JOHNS HOPKINS UNIVERSITY APPLIED PHYSICS LAB ATTN MP3-W110 A GOLDBERG 11100 JOHNS HOPKINS RD LAUREL MD 20723-6099
1	UNIVERSITY OF ARIZONA COLLEGE OF OPTICAL SENSORS ATTN S TYO TUCSON AZ 85721
1	MONTANA STATE UNIVERSITY ATTN J SHAW 108 CULBERTSON HALL P.O. BOX 172000 BOZEMAN MT 59717-2000
1	UNIVERSITY OF ARIZONA ATTN COLLEGE OF OPTICAL SCIENCES B M RATLIFF TUSCON AZ 85721

NO. OF COPIES	ORGANIZATION
2	POLARIS SENSOR TECHNOLOGIES INC ATTN D B CHENAULT ATTN J L PEZZANITI 200 WESTSIDE SQUARE STE 320 HUNTSVILLE AL 35801
1	US ARMY RSRCH LAB ATTN RDRL CIM G T LANDFRIED BLDG 4600 ABERDEEN PROVING GROUND MD 21005-5066
15	US ARMY RSRCH LAB ATTN IMNE ALC HRR MAIL & RECORDS MGMT ATTN RDRL CIE M FELTON (5 copies) ATTN RDRL CIE S K GURTON (5 copies) ATTN RDRL CIM L TECHL LIB ATTN RDRL CIM P TECHL PUB ATTN RDRL SEE E K KLETT ATTN RDRL SES E D ROSARIO

TOTAL: 36 (1 ELEC, 1 CDS, 34 HCs)